

## A POTENTIAL MATERIAL FOR TISSUE ENGINEERING: SILKWORM SILK/PLA BIOCOMPOSITE

Hoi-Yan Cheung<sup>1</sup>, Kin-Tak Lau<sup>1,\*</sup>, Xiao-Ming Tao<sup>2</sup> and David Hui<sup>3</sup>

<sup>1</sup>Department of Mechanical Engineering, <sup>2</sup>Institute of Textiles and Clothing,  
The Hong Kong Polytechnic University,  
Hung Hom, Hong Kong SAR, China

<sup>3</sup> Department of Mechanical Engineering, University of New Orleans,  
New Orleans LA 70148, USA.

\*Corresponding author: [mmktlau@polyu.edu.hk](mailto:mmktlau@polyu.edu.hk)

*Keywords:* Biocomposites, Mechanical properties.

### Abstract

Poly(lactic acid) (PLA), a kind of well recognized bio-degradable polymer, was reinforced by silkworm silk fibers to form a completely biodegradable and biocompatible biocomposite for tissue engineering applications. The influence on the mechanical and thermal properties of the biocomposite in relation to the length and weight content of silk fibers is studied in this paper. Through the micro-hardness test, optimized fiber length and weight content of silk fibers used to make a better strength silk fiber/PLA biocomposite was determined. Tensile property test and thermal analyses including differential scanning calorimetry (DSC), dynamic mechanical analysis (DMA) and thermogravimetry analysis (TGA) for the silk fiber/PLA biocomposite with specified fiber length and weight content were then conducted to investigate its property changes in comparison to a pristine PLA sample. Experimentally, it was found that the fiber length and weight content of silk fibers are key parameters that would substantially influence the hardness of the biocomposite samples. For microscopic observations, good wettability of the fibers inside the biocomposite was seen. The surface of the fibers was well bonded with the matrix, as observed by a SEM image of fractured sample. As a result, it was found that the use of silk fibers can be a good candidate, as reinforcements for the development of polymeric scaffolds for tissue engineering applications.

## **1. Introduction**

In general, the development of biomaterials begins with those bioinert materials such as metals, ceramics and silicon etc. which are implanted permanently inside the host body without generating any adverse response and interaction with surrounding tissues. Nevertheless, the demand of biocompatible, biodegradable and bioresorbable materials has increased drastically since the last decade. The medical applications of these biomaterials are categorized into six main fields, namely (i) tissue fixation, (ii) tissue regeneration, (iii) anti-tissue adhesion, (iv) wound closure, (v) wound dressing and (vi) drug delivery system. Consequently, a wide variety of natural and synthetic biodegradable polymers have been investigated recently for medical and pharmaceutical applications.

Natural biodegradable polymers like collagen, gelatin, chitosan and hyaluronic acid etc. have been studied for various medical applications. However, their high cost and questionable purity have limited their applications. On the contrary, synthetic biodegradable polymers, thermoplastic aliphatic poly(esters) like poly(lactic acid) (PLA), poly(glycolic acid) (PGA) and their copolymers etc., are man-made polymers. They have a promising advantage over natural polymers for the implant development because of their favorable properties, including good biocompatibility, biodegradability, bioresorbability, and mechanical and proliferation properties, are more predictable and reproducible. Their physical and chemical properties can be easily modified to achieve desirable mechanical and degradation characteristics. Additionally, synthetic polymers are generally degraded by simple hydrolysis, which is desirable as their degradation rate do not have variations from host to host, unless there are inflammations and implant degradation to affect local pH variations. They possess low or even negligible toxicity of products during in vivo degradation.

Among various synthetic biodegradable polymers, PLA is particularly offering increasing commercial interest since it is now possible to obtain high molecular weight PLA with expected lifetime by industrial technologies. Additionally, PLA can maintain its mechanical properties, even under a humid environment without being suffered for rapid hydrolysis, and thus, PLA can be a potential structural material. PLA is a highly versatile biopolymer derived from renewable resources like starch or

sugar-based materials such as corn [1]. This biodegradable polymer is alpha polyester that is widely used in medical applications and it has been approved by Food and Drug Administration (FDA) for implantation in human body. During biodegradation, PLA degrades into lactic acid which is finally metabolized and excreted from the host as carbon dioxide and water.

Biocomposites mainly consist of biopolymers reinforced by natural/bio-fibers which are classified into plant-based and animal-based fibers. Silkworm silk fiber is one of the animal-based natural fibers which is a potential candidate for structural composites and can be used for various medical applications such as wound sutures and biomedical scaffolds. In modifying the thermal and mechanical properties of biodegradable polymers, silk-based fiber reinforced polymeric composites have emerged recently [2-7]. As referred to those literatures, epoxy and natural or synthetic biodegradable polymers such as alginate and poly(butylene succinate) (PBS) were mainly used as matrix for the composites. For PLA, several studies have reported that traditional synthetic fibers, like glass and recycled newspaper fibers, and plant-based natural fibers, like abaca and bamboo fibers, were used as reinforcements to enhance its mechanical properties. However, only few researches have attempted to use animal-based natural fibers as reinforcements for this biodegradable polymer [8-11].

Experimental data from preceding studies [3,4] tended to support that the use of silkworm silk fibers as reinforcements is able to enhance the mechanical properties of polymeric materials. Several research achievements have developed a conceptual framework for silk-based polymeric composites to be a promising candidate for wide variety of structural applications. Previous researches investigated the impact of silk fibers upon polymeric materials and gave attention to the development of fully biodegradable biocomposites. The purpose of this study is to advance the understanding of the mechanical and thermal properties of a silk fiber reinforced PLA biocomposite (hereafter called “the biocomposite”) through different mechanical and thermal property tests and analyses, such as differential scanning calorimetry (DSC), thermogravimetric analysis (TGA) and dynamic mechanical analysis (DMA) to investigate the glass transition, melting and decomposition temperatures, thermal stability, and dynamic loss modulus, dynamic loss modulus and tangent delta as a function of temperature and frequency of the biocomposite respectively for tackling

the thermal stability problems of biodegradable polymers. Besides, the enhancement of mechanical properties of PLA with the use of silk fibers was examined by undergoing micro-hardness and tensile property tests. Last but not the least, the morphology of fracture surfaces of the silk fiber/PLA biocomposite was observed by imaging technique with the help of scanning electron microscope (SEM) under ambient temperature to analyze interfacial bonding properties between the silk fibers and PLA matrix.

## **2. Experimental Procedures**

### **2.1 Preparation of composites**

Natural tussah or raw continuous silkworm silk fibers were used as reinforcements for pure PLA to fabricate a completely biodegradable biocomposite. Silkworm silk fibers (hereafter called “the silk fibers”) were cut gently into short fibers in the length of 3, 4, 5, and 6 mm in order to make sure that the fibers were not stressed plastically during the fabrication process. In order to examine an optimal amount of the silk fibers should be used, the fiber weight content of 1, 3, 5 and 7 wt % with different fiber lengths were used for each set of samples. PLA that was supplied by East Link Degradable Materials Ltd., Hong Kong, was used as matrix in this study. Before fabricating the biocomposites, the silk fibers and PLA pellets first underwent a dry treatment with heat applied (80 °C) for 24 hours in an oven so as to remove excessive moisture. Otherwise, the properties of PLA would be strongly affected due to the formation of voids after curing.

In this study, the comparison of the mechanical and thermal properties of the biocomposites and pure PLA samples were made. All sets of samples were fabricated by extrusion and injection molding method to ensure that consistent results were received. The silk fibers and PLA matrix were mixed at the different ratios of 1:99, 3:97, 5:95 and 7:93, fed into a Hakke MiniLab twin-screw micro extruder and a uniform temperature of 183 °C was maintained at all zones inside the machine. The screw speed and the mixing duration were set to 100 rpm and 10 minutes, respectively. The first run of the extrusion was discarded and the strands of the extrusion products were then directly collected by a pre-heated injection cylinder for further injection molding. The molten mixture was then transferred to a Thermo Hakke small scale

injection-molding machine; the injection cylinder and the mold were pre-heated to desired temperatures of 200 °C and 45 °C respectively. The resultant biocomposite samples were in a dumbbell shape according to ASTM D638.

## **2.2 Measurements**

Micro hardness test was performed to determine optimal fiber length and weight content by means of comparing the hardness between the pure PLA and biocomposite samples. The test was done by the Vickers hardness tester (Future-tech FM series). The loading force and dwelling time were set as 100 gram force and 15 seconds respectively. Since the injection molded samples were both sided polished and flattened, further surface finishing processes could be neglected. Samples were randomly selected, and 5 points were dwelled on each sample for averaging the results to maintain accuracy.

A tensile test was then carried out in order to examine the mechanical properties of pure PLA and silk fiber/PLA biocomposite according to the ASTM standard by using the 50 kN MTS Alliance RT-50 tensile machine and extensometer. In order to maintain the accuracy of measurement, all testing samples were molded into a dumbbell shape and underwent the same ambient testing conditions. The span length was 50 mm, and crosshead speed with a loading rate of 2 mm/min was used. 10 samples for each of the pure PLA and silk fiber/PLA biocomposite were tested.

DSC was used to characterize the melting points, glass transition temperatures, and other material and material reaction characteristics such as specific heat, crystallinity, and reaction kinetics of all samples. In this study, the melting and crystallization behavior of pure PLA and silk fiber/PLA biocomposite were studied by using the Perkin-Elmer DSC7 system at ambient condition. The temperature range of the experiment was programmed to start at 25 °C and end at 300 °C at a constant scanning rate of 10 °C/min. All the samples with sample weight of approximately 5 mg were placed and sealed into an aluminium pan, and an empty aluminium pan which has the same weight as the sample pan was used as reference. The heat flow and energy changes in the aluminium pans were recorded. By observing the difference in heat flow between the samples and the reference sample, DSC was able to measure the

amount of energy absorbed or released during the samples' phase transition. Therefore, crystallization and melting temperatures could be read from the peaks as shown on the graphs, and even more subtle phase changes like glass transition temperature ( $T_g$ ) could be observed.

DMA is a technique in which the elastic and viscous responses of a sample under oscillating load are monitored against temperature, time or frequency where the frequency of oscillation is proportional to the modulus (stiffness) of the material. Properties obtained from DMA as a function of temperature including storage modulus ( $E'$  or  $G'$ ), which is a measurement of energy stored during deformation and related to solid-like or elastic portion of the elastomer, loss modulus ( $E''$  or  $G''$ ), which is a measurement of energy lost, usually as heat, during deformation and related to liquid-like or viscous portion of the elastomer, and tangent delta ( $\tan \delta$ ), which is related to material's ability to dissipate energy in the form of heat. Elastomer melting point ( $T_m$ ) and glass transition temperature ( $T_g$ ) can also be determined from DMA curves. Here the Perkin Elmer Diamond DMA Lab System was set to scan thermally from 25 °C to 100 °C with a scanning rate of 2 °C/min. Sinusoidal oscillation of 1 Hz was selected. According to the specifications provided, for a dual-cantilever bending test, the sample was processed to 50 mm in length, 5 mm in width and 1.5 mm in thickness with both ends clamped. A load was applied in the middle of the sample.

Thermal stability of both the pure PLA and silk fiber/PLA biocomposite were revealed by making use of the Setaram Labsys TG-DTA/DSC (the accuracy was  $\pm 1 \mu\text{g}$ ) system at ambient condition. The temperature was set to start at 25 °C and end at 500 °C with the temperature scanning rate of 10 °C/min, and air flow rate was set to be around 400 cc/min. Changes in weight percentage during temperature scanning and the decomposition temperatures of the materials can be determined.

After the thermal and mechanical property tests, microscopic analysis with the help of Leica Stereoscan 440 scanning electron microscope (SEM) was conducted on fracture surface of the samples to examine the failure surface structure and failure behavior induced by tensile test. Testing was performed at room temperature with tungsten filament, and an accelerating voltage of 20 kV was used to capture SEM images for

both of the pure PLA and silk fiber/PLA biocomposite. All specimens were viewed perpendicular to the fractured surface.

### 3. Results and Discussion

#### 3.1 Hardness Test

Vickers hardness test was performed to determine the micro-hardness of the pure PLA and biocomposite samples with different fiber lengths and weight contents. After averaging the measured results, the hardness of the pure PLA is 17 Hv, whereas the results for biocomposite samples with different fiber length and weight content are plotted in Figure 1. In the figure, it is obviously seen that with increasing the length of the fibers from 3 mm to 5 mm, the hardness increases accordingly. However, the reduction of the hardness is observed when the fiber's length beyond 5 mm for all the biocomposite samples with different fiber weight contents (from 1 wt. % to 6 wt. %). An attempt of making a sample with the fiber weight content of 7 wt. % was conducted; however, it was found that the sample was relatively brittle and hardly demolded. Therefore, the maximum viable amount of the fiber for practical applications, to be used to make the biocomposite was 6 wt. %.

In the figure, it also indicates that an optimal fiber length and weight content, that can be used to produce a better strength biocomposite are 5 mm and 5 wt. %, respectively. The maximum hardness of 19 Hv is seen in the figure. For the sample with the same fiber weight content, any increment of the fiber length would result in decreasing the amount of the fibers used inside the biocomposite, and thus, the stress transferability inside the biocomposite may be reduced due to the distance between the fibers decreases, i.e. work done will be gone to the deformation of matrix rather than fibers.

The yield strength of materials can be approximated by using Eq. 1, with  $c$  being a constant determined by geometrical factors which is usually ranged between 2 and 4. The results obtained from tensile test show that the yield strength of the pure PLA and silk fiber/PLA biocomposite with 5 wt. % of fibers are consistent with the results obtained from the Vickers hardness test, as

$$H_v = c\sigma \quad (1)$$

The hardness increases as the PLA was reinforced with the silk fibers and there is an increment of about 12 % in hardness of PLA with the reinforcement of silk fibers with the fiber length of 5 mm and weight content of 5 wt. %.

### **3.2 Tensile Test**

The mechanical properties of pure PLA and biocomposite samples were compared by making use of traditional tensile property test. Based on the result obtained from micro-hardness test, the optimized fiber length and weight content of 5 mm and 5 wt. % respectively were used to make a silk fiber/PLA biocomposite for the tensile test. Sufficient amount of specimens in dumbbell shaped were measured according to ASTM standard, and it was found that the results obtained were consistent and could be reproduced well by the extrusion and injection molding technique. The stress-strain curves of the pure PLA and silk fiber/PLA biocomposite are as shown in Figure 2, and the characteristics of the two different composition samples, including peak stress, strain percentage at break and modulus of elasticity, are listed in Table 1. The average tensile strength and the strain percentage at break of the pure PLA are about 65.19 MPa and 6.73% respectively; whereas for the silk/PLA biocomposite sample, the measured results are about 62.08 MPa and 10.29 % respectively. The elastic moduli of the pure PLA and silk/PLA biocomposite samples are 1.83 GPa and 2.54 GPa respectively.

As seen from the peak stress, the tensile strength of the silk/PLA biocomposite is slightly lower than that of the pure PLA. As all silk fibers were randomly oriented inside the biocomposite, the failure of the biocomposite might be initiated by the failure of the matrix and then followed by fiber breakage. Unlike uni-directional fibre-reinforced composites, all stress along the fiber direction would be directly transferred from the matrix to the fibers during loading condition. However, for the strain percentage at break and modulus of elasticity of the silk fiber/PLA biocomposite, increments of up to 53 % and 39 % were obtained respectively. It means that the ductility of the silk fiber/PLA biocomposite was higher than that of the pure PLA. In Figure 2, it is also seen that after the peak stress, the stress-strain curve of the silk fiber/PLA biocomposite is dissimilar to the curve for the pure PLA. A plateau is



located between a strain where the peak stress is reached and the strain at break. It is not hard to anticipate that the failure process of the silk fiber/PLA biocomposite was governed by the bridging effect attributed by the silk fibers inside the biocomposite. The silk fibers, acted as micro-pins to generate the interlocking mechanism inside the matrix, which resulted in prolonging the fracture process of the silk fiber/PLA biocomposite. Apart from the strain percentage at break, the stiffness of the silk fiber/PLA biocomposite was satisfactorily improved when compared to the pure PLA. Thus, the overall mechanical properties of the silk fiber/PLA biocomposite according to the tensile and micro hardness tests were enhanced. These findings could be explained by the fractured morphology of the microstructures inside the samples, which were observed by making use of the SEM.

### **3.3 Crystallization and melting behavior of PLA and silk/PLA biocomposite**

According to the literature reference [12], assuming that PLA is purely crystalline, the value of melting enthalpy of the pure PLA is approximately 93 J/g, so the degree of crystallinity ( $X\%$ ) in the biocomposite can be obtained by:

$$X\% = \Delta H_m / \Delta H_{mo} \times 100\%, \quad (2)$$

in which  $\Delta H_m$  is the measured melting enthalpy and  $\Delta H_{mo}$  is the melting enthalpy value of the purely crystalline sample. All the measured results from DSC testing are summarized in Table 2 and plotted in Figure 3, the values of  $T_g$  for the pure PLA and silk/PLA biocomposite were 60.2 °C and 64.4 °C respectively, with an increment of 7 %. For  $T_m$  and  $\Delta H_m$ , both of the pure PLA and silk fiber/PLA biocomposite are around 170 °C and 35 J/g respectively, and they are quite close to each other, whereas for the crystallization temperature ( $T_c$ ) and crystallization enthalpy ( $\Delta H_c$ ), the values decreased with the addition of silk fibers, and the decrements are dropped by about 14 °C and 15 J/g respectively. Moreover, the degree of crystallinity increased slightly in the presence of silk fibers, and the value was about 38 %.

Two main factors control the crystallization of polymeric composite systems: (i) the additives hinder the migration and diffusion of polymer molecular chains to the surface of the growing polymer crystal in the composites, thus providing a negative

effect on polymer crystallization which results in a decrease in the  $T_c$ ; (ii) the additives have a nucleating effect which gives a positive effect on polymer crystallization and leads to an increase in  $T_c$ . However, in this case, the  $T_c$  of the silk fiber/PLA biocomposite dropped by 14 °C. It may be concluded that in the presence of silk fibers, the viscosity of the biocomposite mixture increased, which hindered the migration and diffusion of PLA molecular chains in the biocomposite.

### 3.4 Dynamic Mechanical Properties

As shown in Figure 4, the storage modulus against temperature,  $E'$ , of the silk fiber/PLA biocomposite is higher than that of the pure PLA sample. The modulus increased in the presence of silk fibers, which could be concluded as a combined effect of the fibers embedded in a viscoelastic matrix and the mechanical limitation introduced by the fibers. At high concentration, the fibers reduced the mobility and deformation of the matrix, and in this case, the stress can be transferred from the PLA matrix to the silk fiber reinforcements [13]. Also, it could be observed that the  $E'$  value of both the pure PLA and silk/PLA biocomposite samples dropped drastically between 53 °C and 67 °C which were their glass transition regions. However, in this glassy zone, the contribution of fiber stiffness to the composite modulus was minimal. Normally, short fiber composite properties are governed by the fiber orientation, fiber length distribution, fiber dispersion and fiber-matrix adhesion. When hydrophilic silk fibers were mixed with hydrophobic PLA matrix, even using the extrusion and injection machine with heat and pressure applied, fiber dispersion would be a serious problem to deal with; but still, the stiffness of the biocomposite was increased as  $E'$  increased in this study.

In Figure 5, the comparison of the loss modulus as a function of temperature,  $E''$ , for both the pure PLA and silk fiber/PLA biocomposite are shown. Comparing the  $E''$  peaks of the two different samples, the  $T_g$  of the silk/PLA biocomposite sample is slightly shifted to higher temperature with a broader range of the transition region than the pure PLA. As the loss factors are sensitive to molecular motions, it could mean that the mobility of the polymer molecular chains decreased as the chains were hindered by the silk fiber reinforcements and led to the shift of  $T_g$ . This might be a

trend that as silk fiber weight content increased, the mobility of polymer chains decreased, and  $T_g$  increased subsequently.

According to Figure 6, tangent delta as a function of temperature,  $\tan \delta$ , for both the pure PLA and silk fiber/PLA biocomposite are shown for comparison, from the relationship between  $E'$ ,  $E''$  and  $\tan \delta$  [14], can be calculated as:

$$\tan \delta = E''/E' \quad (3)$$

$\tan \delta$  decreased as seen from the graph in the presence of silk fibers. This might be again due to the decrement of the mobility of polymer molecular chains as hindered by the reinforcements, which led to a reduction of height and sharpness of the peak in the curves. In addition, damping in the transition region measured imperfection in the elasticity, and some of the energy used to deform the material was directly dissipated into heat. Thus, the mechanical loss that overcame the friction of intermolecular chain was reduced with silk fiber additives [15,16]. It was also claimed in another literature that the reduction in  $\tan \delta$  denoted the improvement in hysteresis of the system and a reduction in internal friction [17].

### 3.5 Thermogravimetry

From TGA testing, thermogravimetric (TG) curves and derivative thermogravimetry (DTG) curves as a function of temperature of both the pure PLA and silk fiber/PLA biocomposite were obtained and are shown in Figures 7 and 8. The TG curves indicate the thermal stability of the materials, whereas the DTG curves shows the decomposition temperature of the materials. Generally speaking, silk fibers degrade through three main stages: (i) starting from 52 °C, the moisture absorbed during storage will be released from the silk fibers; (ii) a second transition, from 265 °C to 350 °C, the silk fibers undergo degradation; and (iii) from 350 °C onwards, the silk fibers start to decompose. According to the two figures, both the pure PLA and silk fiber/PLA biocomposite show very similar results and the data of the curves are quite close to each other. In the TG graph, it can be observed that for both the pure PLA and silk fiber/PLA biocomposite, the weight percentage drops significantly starting from 300 °C, which is mainly due to the degradation of the materials. In addition,

another transition starts at around 360 °C when the decomposition of the materials starts. Thermal stability of the silk fiber/PLA biocomposite was enhanced by the silk fiber reinforcements which act as barriers for better heat insulation and lower the volatile degradation products permeation into the biocomposite. Also, it can be observed that the silk fiber reinforcements improved the weight of residues (char) remained at the region after 360 °C. The weight percentage of char remains at 400 °C for pure PLA was about 5 % and for the silk fiber/PLA biocomposite was about 18 %. This enhancement of char formation could be claimed as a high heat resistance exerted by the silk fiber reinforcements. On the other hand, in DTG graph, a gentle declination starts at around 270 °C, which is the same reason for the start of the degradation of the materials. A peak appears at around 350 - 365 °C for both pure PLA and silk fiber/PLA biocomposite, which is the decomposition region of the materials, and that is consistent with the results obtained by the DSC analysis.

### **3.6 SEM**

The morphology of the fracture surface of the silk fiber/PLA biocomposite was investigated through SEM. The fractographs on the fracture surfaces of the pure PLA and silk fiber/PLA biocomposite are shown in Figures 9 to 11. In Figure 9, it illustrates that the topology of the pure PLA is relatively smooth and no voids are observed. Moisture absorption during the manufacturing process did not occur in the sample.

This concludes that the manufacturing process of the sample was in a good condition. As referred to Figure 10, a network formed by silk fibers inside the silk fiber/PLA biocomposite is seen. Such network was able to reinforce the biocomposite during loading condition. The bridging effect was created easily to stop any crack propagation, which is well matched to the result obtained from the tensile test. Fiber fracture is observed during the examination, which reflects that a good interfacial bonding between the fiber and matrix exist in the silk fiber/PLA biocomposite. In Figure 11, a layer of PLA was remaining coated on the surface of a broken silk fiber, it further proves that the bonding of the fibers and PLA matrix was in a good condition after being extruded.

#### **4. Conclusions**

In this paper, the mechanical and thermal properties of a silk fiber/PLA biocomposite were studied through different experimental approaches. Optimal values, in terms of fiber length and weight content of 5 mm and 5 wt. %, respectively to achieve the maximum micro-hardness of the biocomposite were obtained. The tensile property test revealed that the modulus of elasticity and ductility of the biocomposite were substantially increased to 53 % and 39 %, respectively as compared with pure PLA. Besides, the glass transition temperature of the biocomposite increased approximately by 10 %. SEM images also showed that good interfacial bonding between the silk fibers and PLA matrix was achieved, which reflected a good wettability of the resin during injection and extrusion process was resulted.

As PLA has been well recognized as one of the excellent biodegradable and biocompatible materials used for tissue engineering application, its limitation for the real-life practical is mainly due to its low mechanical and thermal properties. In this paper, it proposes a type of biocomposite, made by biodegradable silk fibers and PLA together, to produce its strength and thermal stability better than the host polymeric material for tissue engineering applications. There is no doubt that this biocomposite should be suitable for any man-kind application as both constituents are biodegradable and biocompatible. Further study will be focused on the degradability of the biocomposite in animal body.

#### **Acknowledgement**

This project was supported by The Hong Kong Polytechnic University Grant and Research Grant Council (PolyU 5205/06E and PolyU 5198/07E). The authors also express their appreciation to East Link Degradable Materials Ltd., Hong Kong for supplying poly(lactic acid).

## References

1. Sun X.S.. Plastics derived from starch and poly(lactic acids). In Wool R.P. and Sun X.S. (ed), Bio-based polymers and composites. Elsevier Academic Press, UK, 2005.
2. Priya S.P., Ramakrishna H.V. and Rai S.K.. Tensile, flexural, and chemical resistance properties of waste silk fabric-reinforced epoxy laminates. *Journal of Reinforced Plastics and Composites*. Vol 24, pp 643-648, 2005.
3. Cheung H.Y. and Lau K.T.. Mechanical performance of silk-based structural composites. *Key Engineering Materials*. Vol 326-328, pp 457-460, 2006.
4. Cheung H.Y. and Lau K.T.. Mechanical performance of an animal-based silk/polymer bio-composite. *Key Engineering Materials*. Vol 334-335, pp 1161-1164, 2007.
5. Lee S.M., Cho D.H., Park W.H., Lee S.G., Han S.O. and Drzal L.T.. Novel silk/poly(butylenes succinate) biocomposites: the effect of short fiber content on their mechanical and thermal properties. *Composites Science and Technology*. Vol 65, pp 647-657, 2005.
6. Han S.O., Lee S.M., Park W.H. and Cho H.. Mechanical and thermal properties of waste silk fiber-reinforced poly(butylenes succinate) biocomposites. *Journal of Applied Polymer Science*. Vol 100, pp 4972-4980, 2006.
7. Lee K.G., Kweon H.Y., Yeo J.H., Woo S.O., Lee J.H. and Park Y.H.. Structural and physical properties of silk fibroin/alginate blend sponges. *Journal of Applied Polymer Science*. Vol 93, pp 2174-2179, 2004.
8. Huda M.S., Drzal L.T., Misra M., Mohanty A.K., Williams K. and Mielewski D.F.. A study on biocomposites from recycled newspaper fiber and poly(lactic acid). *Industrial and Engineering Chemistry Research*. Vol 44, pp 5593-5601, 2005.
9. Huda M.S., Drzal L.T., Mohanty A.K. and Misra M.. Chopped glass and recycled newspaper as reinforcement fibers in injection molded poly(lactic acid) (PLA) composites: a comparative study. *Composites Science and Technology*. Vol 66, pp 1813-1824, 2006.
10. Shibata M., Ozawa K., Teramoto N., Yosomiya R. and Takeishi H.. Biocomposites made from short abaca fiber and biodegradable polyesters.

- Macromolecular Materials Engineering. Vol 288, pp 35-43, 2003.
11. Lee S.H. and Wang S.. Biodegradable polymers/bamboo fiber Biocomposite with bio-based coupling agent. *Composites: Part A*. Vol 37, pp 80-91, 2006.
  12. Nam J. Y., Raya S.S. and Okamoto M.. Crystallization behavior and morphology of biodegradable polylactide/layered silicate nano-composite. *Macromolecules*. Vol 36, pp 7126-7131, 2003.
  13. Rana A.K., Mitra B.C. and Banerjee A.N.. Short jute fiber-reinforced polypropylene composites: dynamic mechanical study. *Journal of Applied Polymer Science*. Vol 71, pp 531-539, 1999.
  14. Groenewoud W.. *Characterisation of Polymers by Thermal Analysis*. Elsevier Science B.V., The Netherlands, 2001.
  15. Bleach N.C., Nazhat S.N., Tanner K.E., Kellomaki M. and Tormala P.. Effect of filler content on mechanical and dynamic mechanical properties of particulate biphasic calcium phosphate-polylactide composites. *Biomaterials*. Vol 23, pp 1579-1585, 2002.
  16. Pothan L.A., Oommen Z. and Thomas S.. Dynamic mechanical analysis of banana fiber reinforced polyester composites. *Composites Science and Technology*. Vol 63, pp 283-293, 2003.
  17. Fay J.J., Murphy C.J., Thomas D.A. and Sperling L.H.. Effect of morphology, cross-link density, and miscibility on inter-penetrating polymer network damping effectiveness. *Polymer Engineering Science*. Vol 31, pp 1731-1741, 1991.

## List of tables and figures

- Table 1. Tensile strength, ductility and modulus of elasticity of pure PLA samples and 5 wt% silk/PLA biocomposites
- Table 2. Thermal properties of pure PLA sample and 5wt% silk/PLA biocomposite by the use of DSC
- Figure 1. Micro hardness test results on different fiber length and content of silk/PLA biocomposite
- Figure 2. Stress-strain curves of (a) pure PLA sample; (b) 5 wt% silk/PLA biocomposite
- Figure 3. DSC curves of (a) pure PLA sample; (b) 5 wt% silk/PLA biocomposite
- Figure 4. Storage modulus as a function of temperature of (a) pure PLA sample; (b) 5 wt% silk/PLA biocomposite
- Figure 5. Loss modulus as a function of temperature of (a) pure PLA sample; (b) 5 wt% silk/PLA biocomposite
- Figure 6. Tangent delta as a function of temperature of (a) pure PLA sample; (b) 5 wt% silk/PLA biocomposite
- Figure 7. Thermogravimetric curves as a function of temperature of (a) pure PLA sample; (b) 5 wt% silk/PLA biocomposite
- Figure 8. Derivative thermogravimetry curves as a function of temperature of (a) pure PLA sample; (b) 5 wt% silk/PLA biocomposite
- Figure 9. SEM micrographs of the fracture surface of pure PLA samples
- Figure 10. SEM micrographs of the fracture surface of 5 wt% silk/PLA biocomposites
- Figure 11. SEM micrographs of the fracture surface of silkworm silk fiber in 5 wt% silk/PLA biocomposites



Table 1. Tensile strength, ductility and modulus of elasticity of pure PLA samples and 5 wt% silk/PLA biocomposites

Samples	Peak Stress (MPa)	Strain percentage at break (%)	Modulus of elasticity (GPa)
Pure PLA	65.19	6.73	1.83
5 wt% silk/PLA	62.08	10.29	2.54

Table 2. Thermal properties of pure PLA sample and 5wt% silk/PLA biocomposite by the use of DSC

Sample / Biocomposite	T <sub>g</sub> (°C)	T <sub>c</sub> (°C)	T <sub>m</sub> (°C)	ΔH <sub>c</sub> (J/g)	ΔH <sub>m</sub> (J/g)	X%
Pure PLA	60.2	114.0	166.5	34.5	35.4	38.1
5 wt% silk/PLA	64.4	100.5	168.4	19.9	35.7	38.4

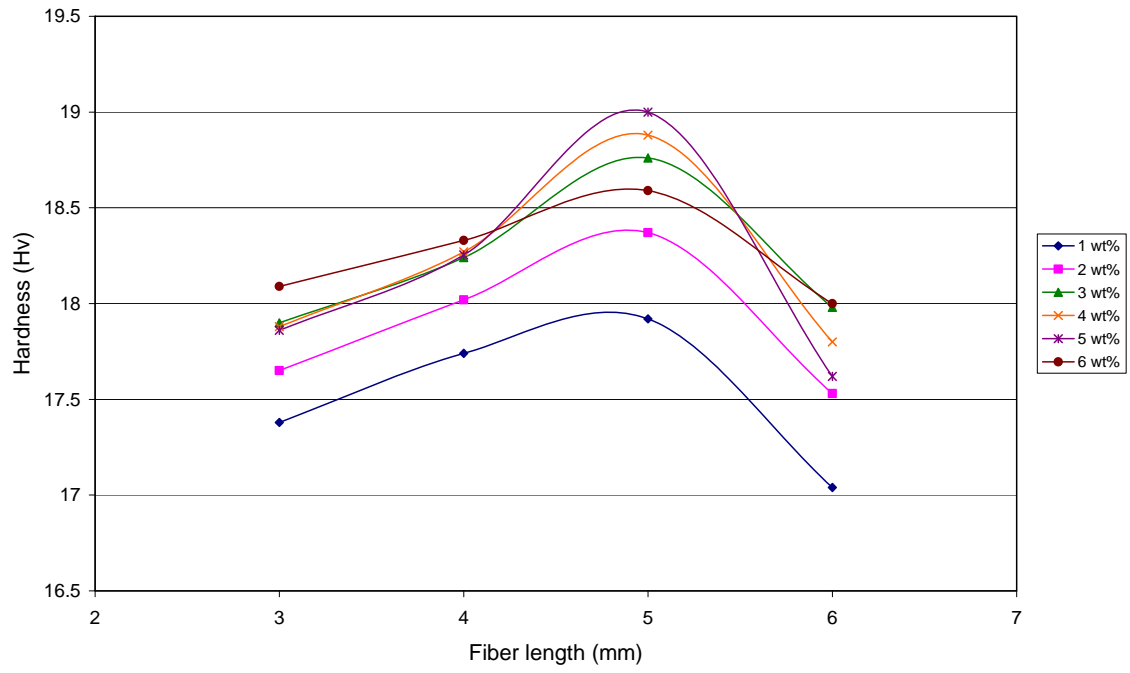


Figure 1. Micro hardness test results on different fiber length and content of silk/PLA biocomposite

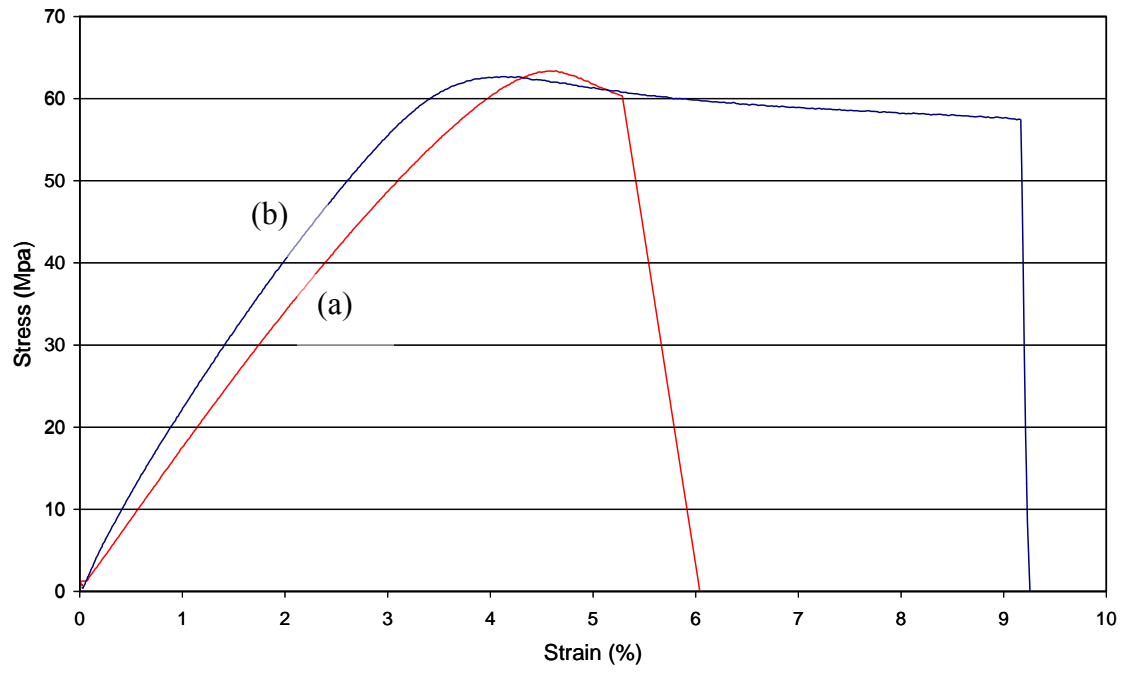


Figure 2. Stress-strain curves of (a) pure PLA sample; (b) 5 wt% silk/PLA biocomposite

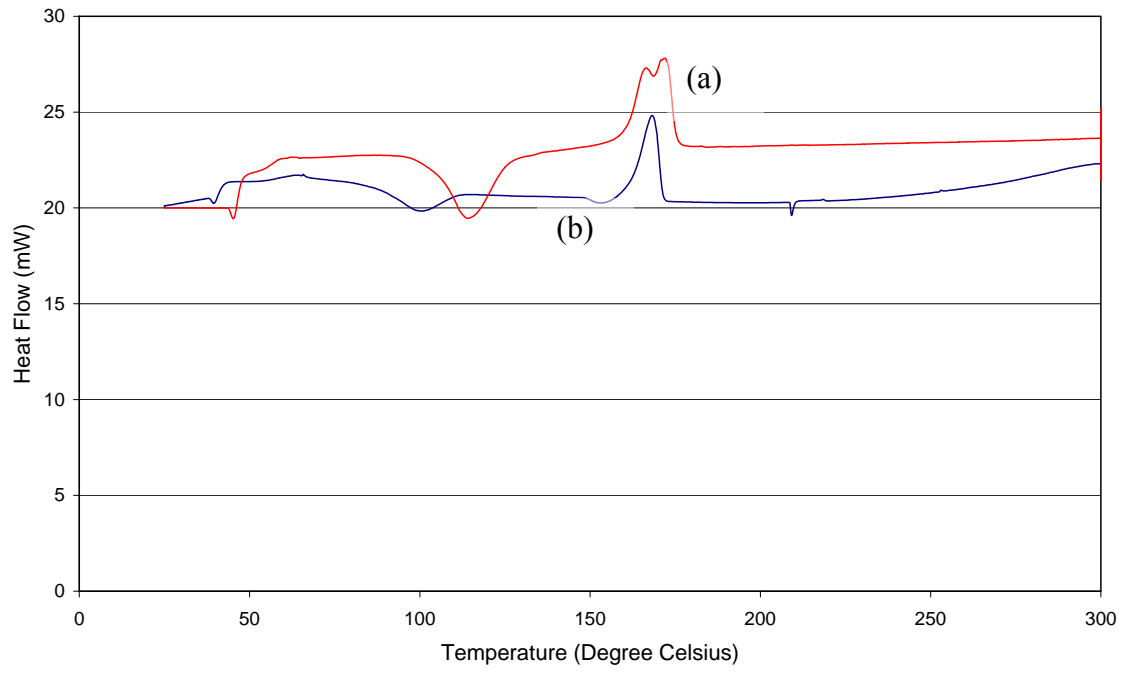


Figure 3. DSC curves of (a) pure PLA sample; (b) 5 wt% silk/PLA biocomposite

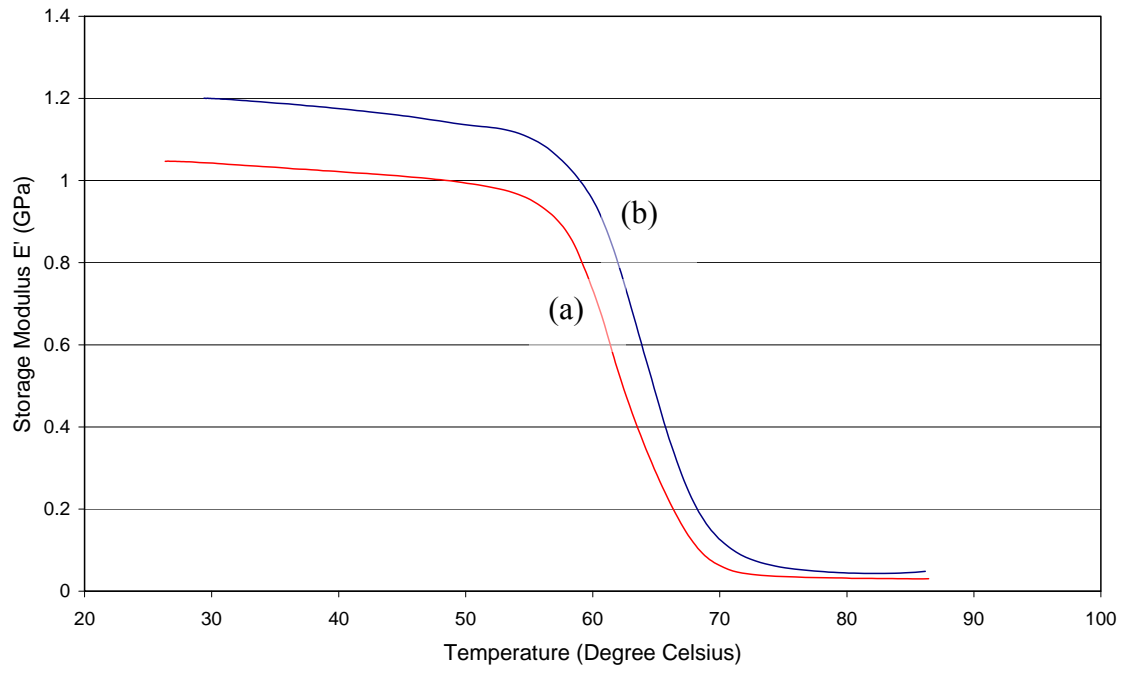


Figure 4. Storage modulus as a function of temperature of (a) pure PLA sample; (b) 5 wt% silk/PLA biocomposite

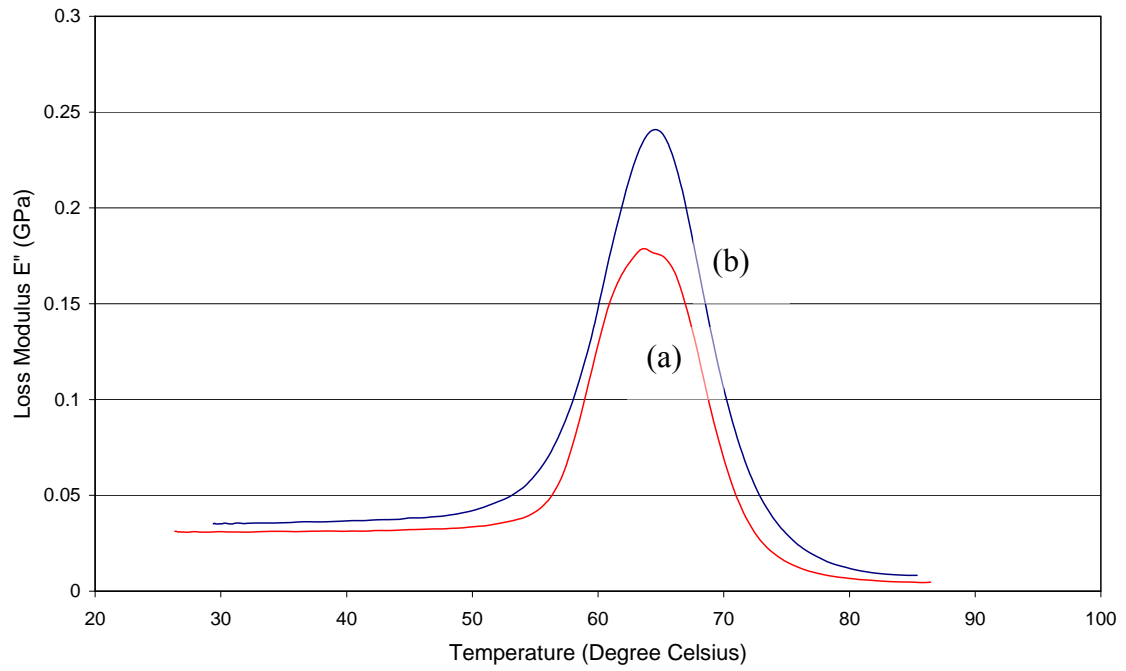


Figure 5. Loss modulus as a function of temperature of (a) pure PLA sample; (b) 5 wt% silk/PLA biocomposite

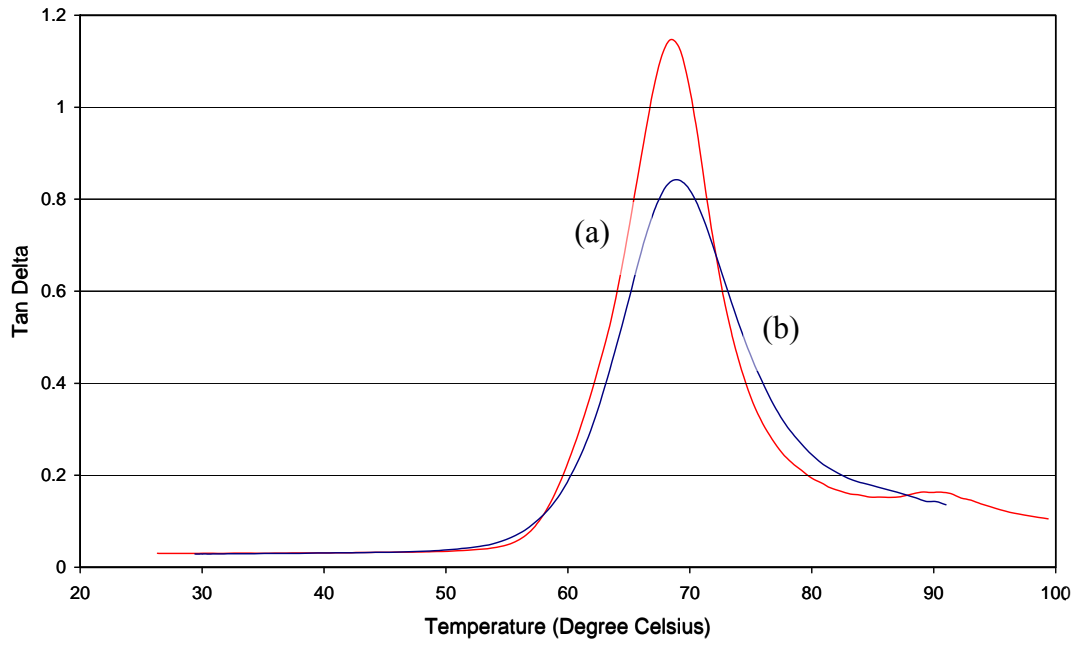


Figure 6. Tangent delta as a function of temperature of (a) pure PLA sample; (b) 5 wt% silk/PLA biocomposite



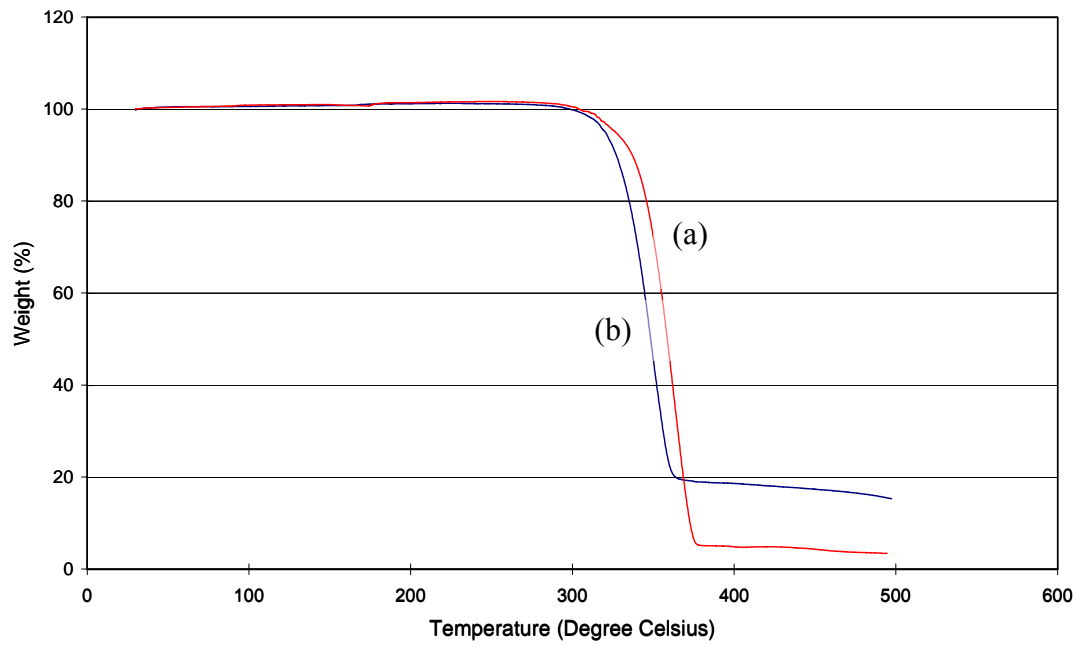


Figure 7. Thermogravimetric curves as a function of temperature of (a) pure PLA sample; (b) 5 wt% silk/PLA biocomposite

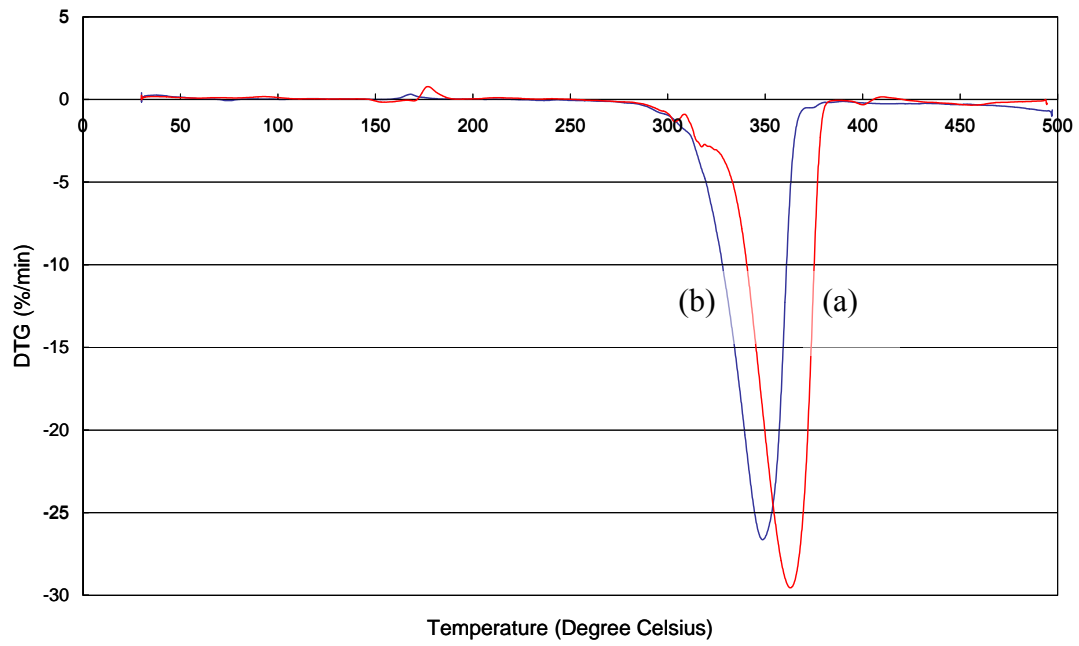


Figure 8. Derivative thermogravimetry curves as a function of temperature of (a) pure PLA sample; (b) 5 wt% silk/PLA biocomposite

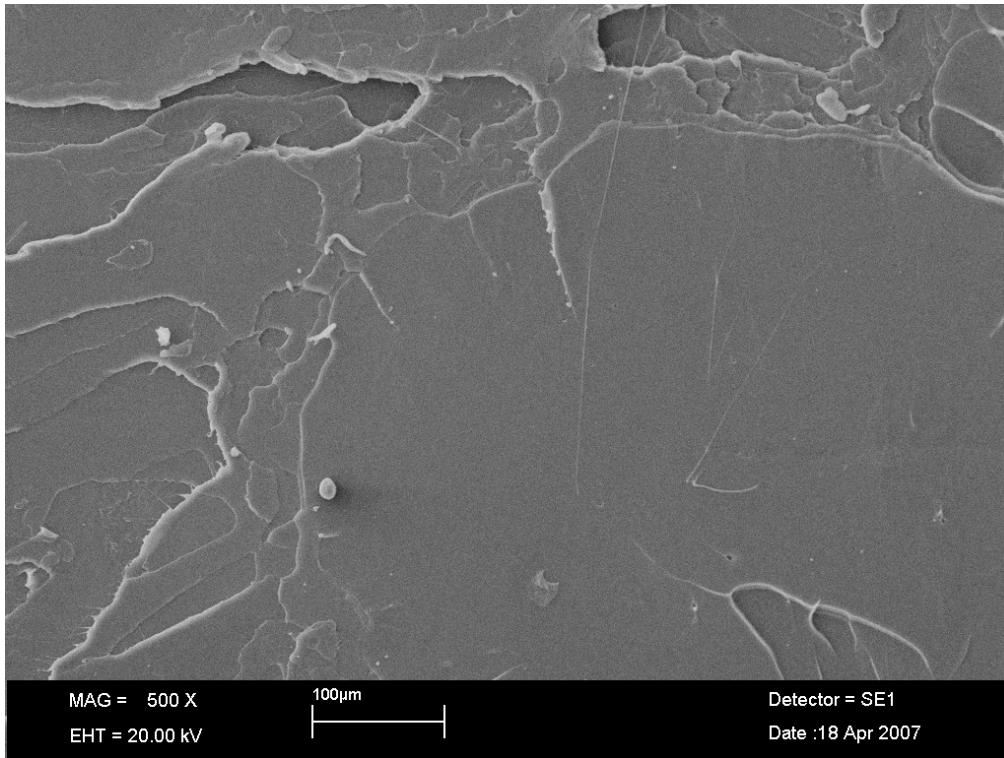


Figure 9. SEM micrographs of the fracture surface of pure PLA samples

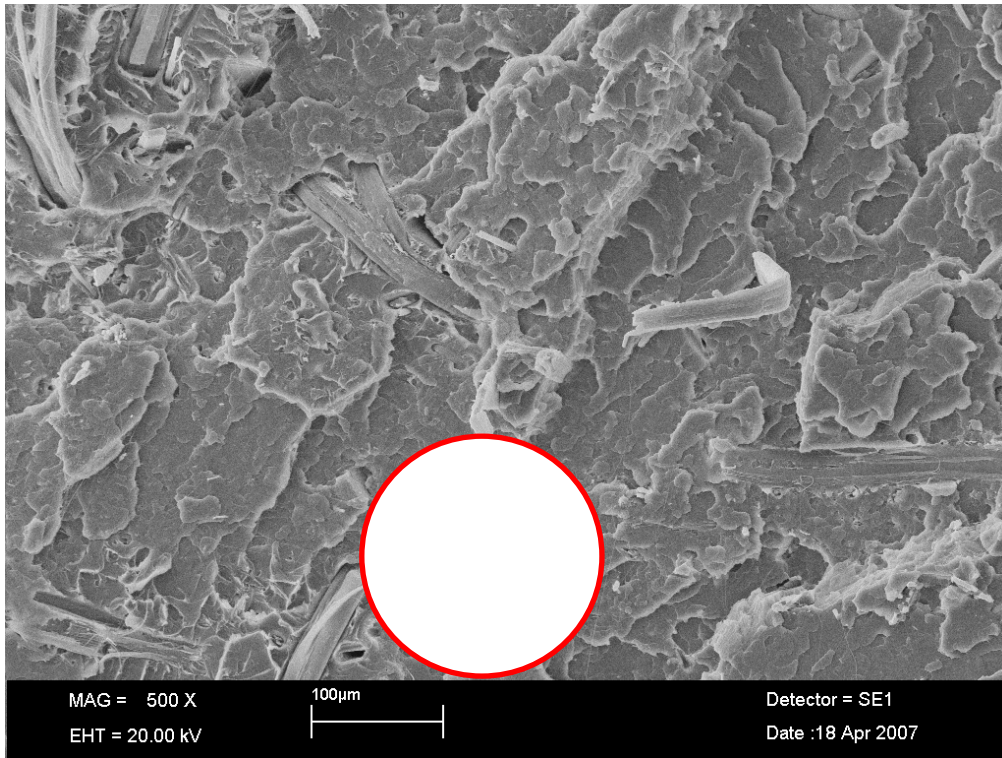


Figure 10. SEM micrographs of the fracture surface of 5 wt% silk/PLA biocomposites

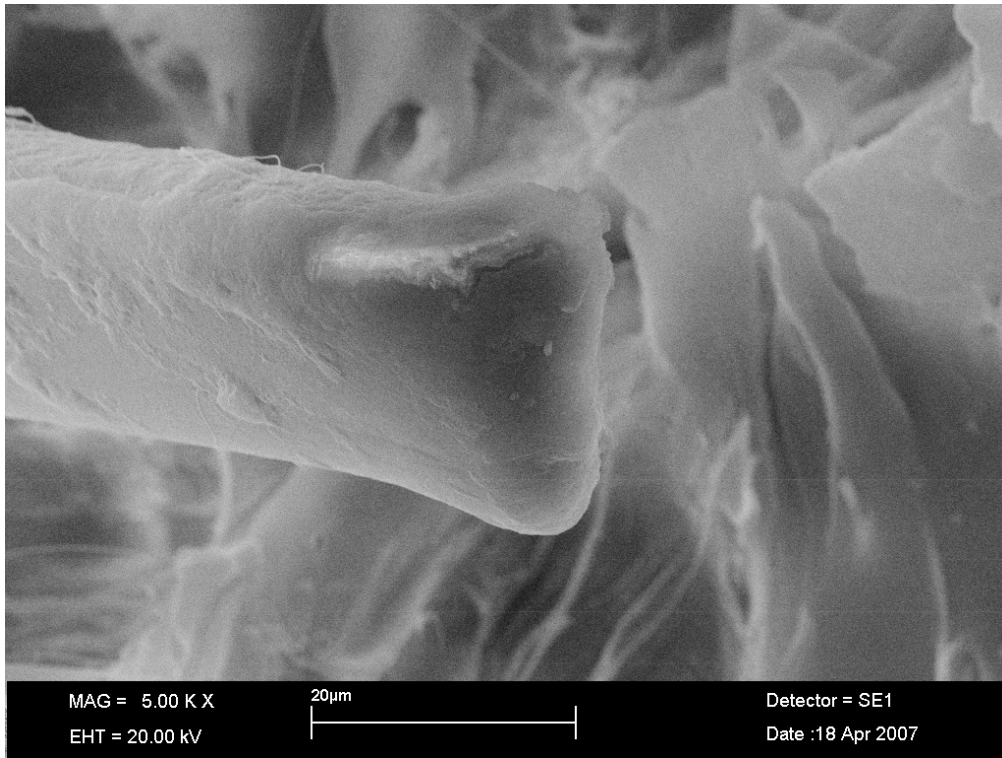


Figure 11. SEM micrographs of the fracture surface of silkworm silk fiber in 5 wt% silk/PLA biocomposites